A physics-based view of brain-network alteration in neurological disease

Sofia Fazio[1], Patrizia Ribino[2], Francesca Gasparini[3,4], Norbert Marwan[5,6,7], Peppino Fazio[8,9], Marco Gherardi[1] and Maria Mannone[2,5,6,8,*]

[1]*Dipartimento di Fisica, Università Statale di Milano, Italy*
[2]*Istituto di Calcolo e Reti ad Alte Prestazioni (ICAR), Consiglio Nazionale delle Ricerche (CNR)*
[3]*Dipartimento di Informatica, Sistemistica e Comunicazione, Università degli Studi di Milano-Bicocca*
[4]*NeuroMI, Milan Center for Neuroscience, Piazza dell'Ateneo Nuovo 1, 20126, Milano, Italy*
[5]*Potsdam Institut für Klimafolgenforschung (PIK), Member of the Leibniz Association, Germany*
[6]*Institute of Physics and Astronomy, Universität Potsdam, Germany*
[7]*Institute of Geosciences Potsdam, Universität Potsdam, Germany*
[8]*Dipartimento di Scienze Molecolari e Nanosistemi (DSMN), Ca' Foscari University of Venice, Italy*
[9]*Department of Telecommunications, VSB - Technical University of Ostrava, Czechia*

Abstract

The brain network damage provoked by a neurological disease can be modeled as the result of the action of an operator, K, acting on the brain, inspired by physics. Here, we explore the matrix formulation of K, analyzing eigenvalues and eigenvectors, with heuristic considerations on different techniques to approximate it. The primary objective of this paper is to lay the foundational groundwork for an innovative framework aimed at the development of predictive models regarding the progression of neurodegenerative diseases. This endeavor will leverage the potential of integrating these novel representations of brain damage with advanced machine-learning techniques. A case study based on real-world data is here presented to support the proposed modeling.

Keywords

Functional network, K-operator, Alzheimer-Perusini's disease progression, predictive models

1. Introduction

Reading the mind has been mankind's dream for centuries. Bridging the gap between physiology and thinking is a related question. Understanding anatomic structures and physiological processes inside the brain is still an ongoing adventure. The association between blood movements and thinking was an intuition of Angelo Mosso [1], who was working with open-skull patients. An intuition that led to the first rough but pioneering system of non-invasive neuroimaging.

HC@AIxIA 2024: 3rd AIxIA Workshop on Artificial Intelligence For Healthcare, Bolzano, Italy, 2024
*Corresponding author.
sofia.fazio@studenti.unimi.it (S. Fazio); patrizia.ribino@icar.cnr.it (P. Ribino); francesca.gasparini@unimib.it (F. Gasparini); marwan@pik-potsdam.de (N. Marwan); peppino.fazio@unive.it (P. Fazio); marco.gherardi@unimi.it (M. Gherardi); {maria.mannone@icar.cnr.it}{maria.mannone@uni-potsdam.de} (M. Mannone)
0000-0002-6769-6642 (S. Fazio); 0000-0003-3266-9617 (P. Ribino); 0000-0002-6279-6660 (F. Gasparini); 0000-0003-1437-7039 (N. Marwan); 0000-0003-2590-034X (P. Fazio); 0000-0002-7745-8269 (M. Gherardi); 0000-0003-3606-3436 (M. Mannone)

In 1890, he developed the so-called *human circulation balance*, a technique that could non-invasively measure the redistribution of blood during emotional and intellectual activity. His experiments provided foundational concepts for modern neuroimaging techniques, highlighting critical variables such as the *signal-to-noise ratio*, the appropriate choice of the experimental paradigm, and the need for the simultaneous recording of several physiological parameters. Understanding the brain processes can also shed light on the mechanisms leading to diseases.

However, for decades, we viewed neurodegenerative disease anatomy through oversimplified frameworks. The beginning of human brain mapping in the late 1980s made it possible through statistical methods to determine disease topographies *in vivo* with network-based representation. Noninvasive and computational methods for modeling the connectivity across the whole brain helped understand the alterations in the brain network architecture [2]. Neuroimaging techniques play a crucial role in the study of neurodegenerative diseases. According to Seeley [3], two key concepts that still lead to many open questions are the onset and progression of these diseases, which have been investigated through the study of *epicenters* whose connectivity in health mirrors the spatial patterning of each syndrome. In light of the studies by Royer and co-authors, atypical hub organization in epilepsy and seizure activity are linked [2]. A network reorganization is also occurring in Alzheimer-Perusini's disease [4]. Using graph theory to study brain networks enabled to calculate topological parameters and identify network hubs [5]; quantifying them using centrality measures allows for investigations of relative differences between different types of epileptic patients and normal controls at the nodal level. Several studies also explored the value of network neuroscience approaches to provide clinically relevant measures in epilepsy, to develop the ability to capture seizures and investigate transient changes in network properties during the generation and evolution of seizures.

In a recent study, Mannone and co-authors [6] represented the damage to the brain network caused by some neurological diseases using a physics-inspired mathematical operator, the *Krankheit*-operator, in short K-operator. When applied to a diseased brain, K describes the progression of the disease over time. The authors also denoted the brain network as a block matrix $\mathcal{G}$, where each diagonal block represents the connections between brain lobes, while the off-diagonal blocks indicate the inter-lobe connections. In a different study, the authors applied this formalism specifically to Alzheimer-Perusini's diseased brains [7].

Starting from [6], the work proposed in this paper explores in detail a mathematical operator computed from the connectivity matrices of the brain functional network, objects with an important potential both in the fields of neurology and artificial intelligence. The proposed study investigates two computational techniques to evaluate the action of the K-operator on the connectivity matrices. The analogies between the two different resulting objects have been analyzed, with a focus on their eigenvalues and eigenvectors. Additionally, a case study based on real-world data has been incorporated into this analysis.

Mainly, the first technique adopts the matrix product for the matrix inversion and the element-wise product for the computation of K. On the contrary, the second technique adopts the usual matrix product for the matrix inversion and K computation.

The rationale for adopting these two different computational techniques lies in their different informational outputs. The first technique provides easily interpretable data regarding which connections between pairs of brain areas are more damaged. In contrast, the second provides precise and cumulative information on the amount of damage.

The data analysis conducted in the real case study underscores the similarities in the information generated by the two distinct techniques.

Building upon these insights, we are establishing the groundwork for an innovative foundational framework aimed at developing predictive models for neurodegenerative diseases. This model primarily aims to integrate the K-operator with advanced machine learning techniques to predict the disease progression in patients at elevated risk. The application of machine learning to brain networks is a promising research field [8], and our work can be integrated within this domain. Our study is a preliminary one, and we will give a first and qualitative glance at the properties of a mathematical object that we will draw from the concept of connectivity matrices.

The article is organized as follows. In Section 2, we describe the formalism. In Section 3, we propose some examples of applications. In Section 4, we discuss a real-data example in light of our findings, and finally, we sketch some possible directions of research (Section 5). For the sake of notation, it is also necessary to stress that, in the following, the *Hadamard* product, also known as element-wise product, usually indicated with $\odot$, will be reported here as $*$, to maintain conformity with the Python code, while the ordinary matrix multiplication will be referred to as @.

2. Formalism and methods

2.1. The K-operator

Let us denote a healthy brain as a block matrix $\mathcal{G}$, where the block on the diagonal represents the connections inside the same lobe, and the others stand for the inter-lobe links. The damage provoked by a brain-based neurological disease can be modeled as the action of the K-operator:

$$K\mathcal{G} = \mathcal{G}^k, \tag{1}$$

where the apex k is a label, and $\mathcal{G}^k$ is the matrix of a brain characterized by disease manifestations [6]. For different diseases, there will be different matrix elements of K. A possible choice for $\mathcal{G}$ is the matrix of weights of the connections between brain hubs. For instance, we can identify these matrices with the connectivity matrices derived from fMRI [7, 9].

We first analyze the action of the K-operator through the computation of $\mathcal{G}^k$ with two different product methods:

$$K * G \qquad K@G \tag{2}$$

first, the so-called element-wise product, denoted by $*$ in Python, and the matrix product, the row-by-column product between matrices, showed as @. In the rest of the article, we will also use these symbols as upper indices to distinguish between the action of K *computed* through the *element-wise* product (Hadamard product) from the K *computed* through the *row-by-column-wise* product (matrix product).

When $\mathcal{G}$, $\mathcal{G}^k$ are known, how can we compute K? We can use a matrix inversion and an appropriate choice of the matrix product, one formally justified (row-by-column), the other yielding a similar sparsity of the results (element-wise). We want to investigate the similarities between these operators.

In the following, we show how K can act in simple cases and how it can be computed through the operation of matrix inversion. We will also analyze its mathematical properties. We consider two different kinds of products here to allow a more intuitive understanding of the action of K.

2.2. Analysis of the K-operator with classic tools of matrix algebra

Let us denote with A, B, C, and D the elements of a 4×4 K-operator. Let a toy $\mathcal{G}$ be defined as another 4×4 matrix, having as diagonal elements (1-element blocks in this initial example) the connectivity inside the frontal lobe f, seen as a whole block, and c, the cerebellum, also seen as a whole block. The off-diagonal elements, also 1-element blocks, are the connectivity between f and c. In a real connectivity matrix, they are equal. If we consider the signal transmission from one area to another, we can separate the pathways according to the direction so that we can distinguish between $f \to c$ and $c \to f$. The K acting row-by-column is defined as follows:

$$K^{@}\mathcal{G} = \begin{pmatrix} A & B \\ C & D \end{pmatrix} \begin{pmatrix} f & fc \\ cf & c \end{pmatrix} = \begin{pmatrix} Af + Bcf & Afc + Bc \\ Cf + Dcf & Cfc + Dc \end{pmatrix}. \tag{3}$$

For the sake of simplicity, let us indicate the inverse of $\mathcal{G}$ as:

$$\mathcal{G}^{-1} = \begin{pmatrix} m & n \\ o & p \end{pmatrix} \tag{4}$$

Using the classical product, and imposing $fc = cf = x$, $K^{@}$ can be obtained as:

$$K^{@} = \mathcal{G}^{k}\mathcal{G}^{-1} = \begin{pmatrix} f^k & x^k \\ x^k & c^k \end{pmatrix} @ \begin{pmatrix} m & n \\ o & p \end{pmatrix} = \begin{pmatrix} f^k m + x^k o & f^k n + x^k p \\ x^k m + c^k o & x^k n + c^k p \end{pmatrix}. \tag{5}$$

2.3. Formal relationship between K computed through two different products in a simple case

If we consider K as a matrix of multiplying factors of the corresponding elements of the brain matrix, its element-wise action can be described as:

$$K^{*}\mathcal{G} = \begin{pmatrix} A' & B' \\ C' & D' \end{pmatrix} \begin{pmatrix} f & fc \\ cf & c \end{pmatrix} = \begin{pmatrix} A'f & B'fc \\ C'cf & D'c \end{pmatrix}. \tag{6}$$

Keeping the idea of the matrix inversion but using the element-wise product, we can develop a mixed technique that yields a symmetric and more easily interpretable form of the K-operator, as follows:

$$K^{*} = \mathcal{G}^{k}\mathcal{G}^{-1} = \begin{pmatrix} f^k & x^k \\ x^k & c^k \end{pmatrix} * \begin{pmatrix} m & n \\ o & p \end{pmatrix} = \begin{pmatrix} f^k m & x^k n \\ x^k o & c^k p \end{pmatrix}. \tag{7}$$

Although we can obtain the K-operator through two different mathematical methods, thanks to the theory of diagonalization of matrices, we can notice some similarities between the computed operators, see Section 4. Analyzing the mathematical properties, such as their eigenvalues and eigenvectors, we can justify the empirical evidence we can see through the simple visualization of K.

We can establish a relationship between K^* and $K^{@}$, defining a suitable T-matrix, such that:

$$K^{@} = K^* + T = \begin{pmatrix} f^k m & x^k n \\ x^k o & c^k p \end{pmatrix} + \begin{pmatrix} x^k o & f^k n + x^k p - x^k n \\ x^k m + c^k o - x^k o & x^k n \end{pmatrix}. \tag{8}$$

2.4. Eigenvalues and eigenvectors

In the context of this first symbolic computation, we can re-write Eq. (8) as:

$$K^{@} = K^* + T = \begin{pmatrix} a & b \\ c & d \end{pmatrix} + \begin{pmatrix} e & f \\ g & h \end{pmatrix}, \tag{9}$$

which yields the eigenvalues:[1]

$$\lambda_{1,2} = \frac{1}{2}\left[\mp\sqrt{(-a-d-e-h)^2 - 4(ad+ah-bc-bg-cf+de+eh-fg)} + a + d + e + h\right] \tag{10}$$

Neglecting the second-order elements depending on parts of the T-matrix, highlighting in bold the residual contribution of T, and re-arranging the terms, the equation reads:

$$\lambda_{1,2} \sim \frac{1}{2}\left[\mp\sqrt{(-a-d)^2 - 4(ad-bc)} + (a+d)\right] + \frac{1}{2}\left(\mathbf{e} + \mathbf{h}\right). \tag{11}$$

Thus, the difference between the eigenvalues of K computed with the two techniques is mostly weighted by the e and h (i.e., $x^k o$ and $x^k n$, respectively), the anti-diagonal elements of K^*.

Concerning the K-operators obtained with the two different methods, we can think of getting $K^{@}$ from K^* with some perturbation that we called T, see Eq. (8). *Perturbation theory* for matrices and linear algebra means estimating the change in the solution to a linear algebra problem caused by a small change in the input [10]. In this case, we can see the difference between the K-operators obtained with the two techniques as a perturbation; this allows us to see one technique as the perturbation of the other.

A detailed study of the perturbation-based approach is out of the scope of this article. In the next section, we propose a sequence of examples to apply in different ways the formalism of the K-operator to some arbitrarily-defined matrices.

3. Toy examples of application

In this section, we analyze some toy examples. In the first one, we will see the action of the K-operator on a healthy brain, modeled in four lobes, where each lobe is composed of 4 *hubs*, each one described by a 4×4 matrix. In the second example, we will see the same action of the K-operator on a healthy brain, but with a simpler and more little model. On the other hand, in the last and third examples, we will see how to obtain K from an inverse operation from the healthy and corrupted networks. What we propose in this analysis are some formal considerations and a qualitative evaluation of the patterns of eigenvalues, belonging to matrices obtained with different computational methods.

[1] Obtained through https://www.wolframalpha.com/

3.1. Given $\mathcal{G}$ and K, find $\mathcal{G}^k$: four lobes, four *hubs*

For a first experimental analysis, let us consider a model representing the healthy brain as a matrix. The K-operator is the action of a disease, while the output is a matrix of the diseased brain. Our healthy matrix is a diagonal block matrix, thus a square matrix 16×16 such that the main diagonal blocks are square matrices, namely A, B, C, D in Eq. (12), each one a 4×4 matrix, while all the off-diagonal blocks as 0-matrices, see Figure 1. Also, the compromised-brain matrix is a diagonal block because K is shaped to act only on the diagonal blocks, this operator is defined according to [6]. The action of K is pictorially represented in Figure 1.

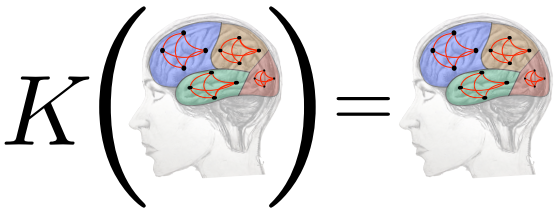

Figure 1: Action of K on a 16×16 simplified brain (neglecting inter-lobe links as in [6]). Drawing by M. Mannone, graphs by S. Fazio.

For our purposes, we define symmetric matrices with 1 along the diagonal to have undirected graphs and the same weights from the j-th node to the i-th and vice-versa. Then, we define the K-operator according to [6], and we compute the matrices related to the diseased brain first applying an element-wise product ($K\mathcal{G}$) and then using the so-called *matrix multiplication*, computed row by column ($K@\mathcal{G}$). The first experimental analysis applied to these product matrices is the computation of their eigenvalues and eigenvectors. From this method, we could infer some analogies between the two techniques, above all among their eigenvalues. The eigenvalues and eigenvectors of the main matrix are simply those of the diagonal blocks combined. It means that when we have the eigenvalues and eigenvectors of A^k, B^k, C^k, D^k, we can also get the ones of the main matrix 16×16 $\mathcal{G}^k$ representing the whole diseased brain, see Eq. (12).

$$K\mathcal{G}|_{\text{no inter-lobe submatrices}} = K \begin{pmatrix} A & & & \\ & B & & \\ & & C & \\ & & & D \end{pmatrix} = \begin{pmatrix} A^k & & & \\ & B^k & & \\ & & C^k & \\ & & & D^k \end{pmatrix} \tag{12}$$

The healthy-brain (sub)matrices are defined with entries' values between 0 and 1, included. Up to a rescaling to $[-1, 1]$, this is coherent with the connectivity matrices and the connections from brains' real data [9]. Our choice is shown in Figure 2 left. Having this knowledge, we should also remember that the matrices that we find through the element-wise products will still have entries between 0 and 1. On the other hand, matrices found with the row-by-column matrix multiplication will admit several entries with values exceeding 1. So, the defined matrices are biologically plausible, considering a normalization. Another noteworthy element is that if we apply a symmetric K to a symmetric $\mathcal{G}$, in the element-wise computation case, we still get a symmetric $\mathcal{G}^k$; while if we get an asymmetric K acting row-by-column, and obtain a

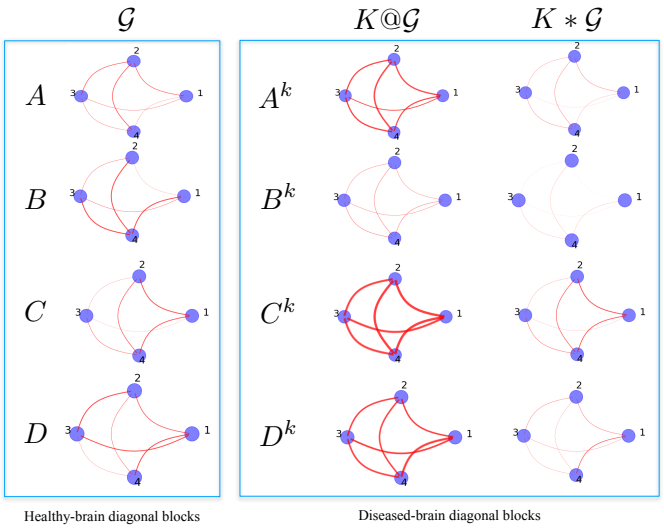

Figure 2: Graphs representing the intra-lobe connections of the healthy brain and of the compromised brain after the application of the K-operator both with the row-by-column matrix multiplication ($@$) and the element-wise product ($*$).

diseased-brain matrix, we notice that the weights between the j-th and i-th and between the j-th and i-th elements (intra-lobe connections) of the matrix are not the same.

The result of the row-by-column and element-wise action of K, yielding the diseased brain (sub)matrices, are shown in Figures 2 center and right, respectively.

3.2. Given $\mathcal{G}$ and K, find $\mathcal{G}^k$: four lobes, one hub per lobe

Let us consider here the case of four lobes, with one hub per lobe, as shown in Figure 3.

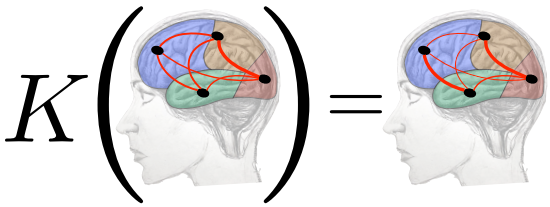

Figure 3: Action of K on a 4×4 simplified brain. Drawing by M. Mannone, graphs by S. Fazio.

As a further example, we choose a different shape of $\mathcal{G}$ and of K to compute $\mathcal{G}^k$ according to the diverse techniques (Figure 4). Here, a 4×4 matrix represents the whole brain to have a more suitable example of application of the theory presented in section 2.4, yet simplified with respect to the example of section 3.1. Darker pixels are in the first column-first row and vice versa, for the results obtained with both techniques. Also, the first eigenvalue is the highest in both cases. Here, we can also see some analogies, above all, among the eigenvalues of the different matrices, even if we chose a simpler model.

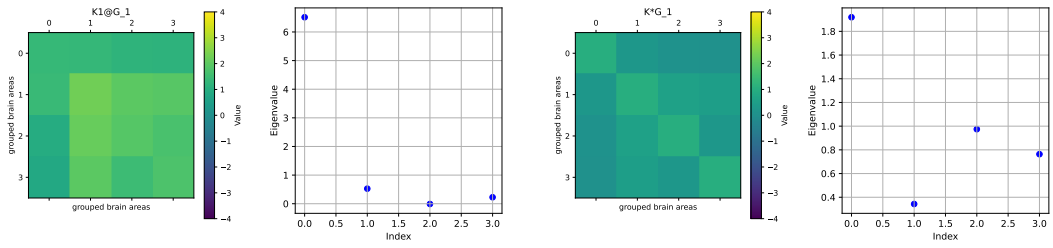

(a) (b) (c) (d)

Figure 4: (a) $K@G$ and eigenvalues (b), $K * G$ (c) and their eigenvalues (d). We notice a vertical correspondence between (a) and (c) and the higher value of the first eigenvalue (b, d).

3.3. Given $\mathcal{G}$ and $\mathcal{G}^k$, find K

In Section 3.1, we defined an example of a simplified healthy brain matrix and an example of the K-operator, computing the diseased brain matrix according to two different kinds of product. In this section, we suppose to know the healthy brain matrix and the diseased one, and we compute K. We exploit the trick of matrix inversion, and compute $K^{@}$ according to classic algebra for a simple 2×2 matrix (Subsection 2.2). Then, we compare the $K^{@}$ with K^{*}, obtained through the element-wise product (Subsection 2.3), and finally, we compute eigenvalues and eigenvectors of the two Ks for a 4×4 brain matrix (Subsection 2.4), and we discuss the possible connections between them. We compare instances of K (Figures 5 and 6). A possible symmetry between the operators can emerge, as we can deduce from the study of eigenvalues and eigenvectors belonging to the K-operator obtained with the two considered methods. Above all, eigenvalues mark some analogies between the different operators.

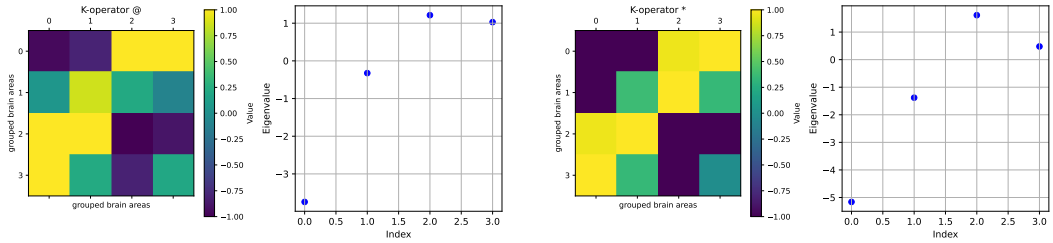

(a) (b) (c) (d)

Figure 5: Two instances of K-operator visualized as heat-maps, computed rows-by-columns (a) and element-wise (c), and the corresponding eigenvalues (b, d).

Our study is the first detailed and eigenvalue-based exploration of the possible analogies between the K-operators acting or computed through two different techniques. For this reason, we focused on eigenvalues, because they allow us to extract information concerning the matrices. So, we collected our observations and we noticed some correspondences and regularities. Further research will aim to develop a theory of a generalized K-operator, and, from the algebraic point

of view, theoretically justifying the correspondences we observed.

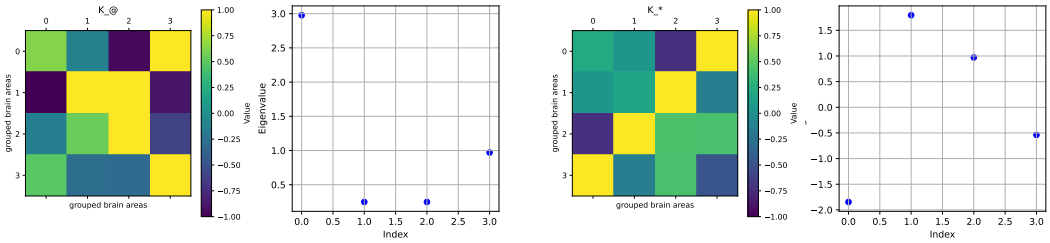

(a) (b) (c) (d)

Figure 6: Other instances of K-operator, rows-by-columns (a) and element-wise (c), and the corresponding eigenvalues (b, d).

4. An example with real data

We can apply the reasoning to one of the patients considered in previous studies, commenting on eigenvalues and eigenvectors of the K-operator derived for real data. We consider a female patient, 56 years old at the baseline, affected by Parkinson's disease [9]. K is derived from the connectivity matrices at the baseline and follow-up, derived from the resting-state functional magnetic resonance rsfMRI_RL, see Figure 7. There are different analysis and processing tools for functional MRI brain imaging data, see for example [11, 12, 13]. For our purposes, fMRI measurements are the starting point for the definition of instances of the K-operator. In particular, we considered the fMRI collected at the baseline and at the first follow-up. We downloaded the corresponding DICOM (Digital Imaging and Communications in Medicine) folder from the PPMI dataset (Parkinson's Progression Markers Initiative),[2] from which we derived the NIfTI file (Neuroimaging Informatics Technology Initiative). Choosing a parcellation of the brain (division into regions of interest), we finally extracted the time series for each region. From the time series for a set of fMRI, we computed the connectivity matrix. Let us now provide some further information on parcellation and connectivity matrices.

The **parcellation** is performed through the choice of an atlas. Among the possible brain atlases, we chose the Automated Anatomical Labeling (AAL3), for the detail provided in limbic and subcortical regions. A detailed analysis of the results that can be obtained with this method in the case of Parkinson's Disease and their medical meaning are discussed in detail in [9]. However, a detailed discussion of them is out of the scope of this article.

A **connectivity matrix** of the brain contains what can be seen as an estimation of the strength of the connections between the specific chosen regions. For different choices of atlases, we get different connectivity matrices. They are, in general, the object of study of several works, where they are specifically analyzed and investigated in detail on their own [14]. However, we are here studying a mathematical object derived from them, the K-operator. From a pair of

[2] https://ida.loni.usc.edu/collaboration/access/appLicense.jsp

connectivity matrices, considering them as the brain matrices characterizing the functional network at two-time points, we compute the K-operator. Our specific example is derived from [9]. We notice that the first eigenvalues are higher, also in the case of a larger matrix and real data, as it can be seen from Figure 7. This confirms our observation for small matrices of synthetic data, considered in the previous Sections. In addition, observing the two K matrices (a, c) in Figure 7, it seems that the first was cut and partially mirrored, to yield the symmetry of the second.

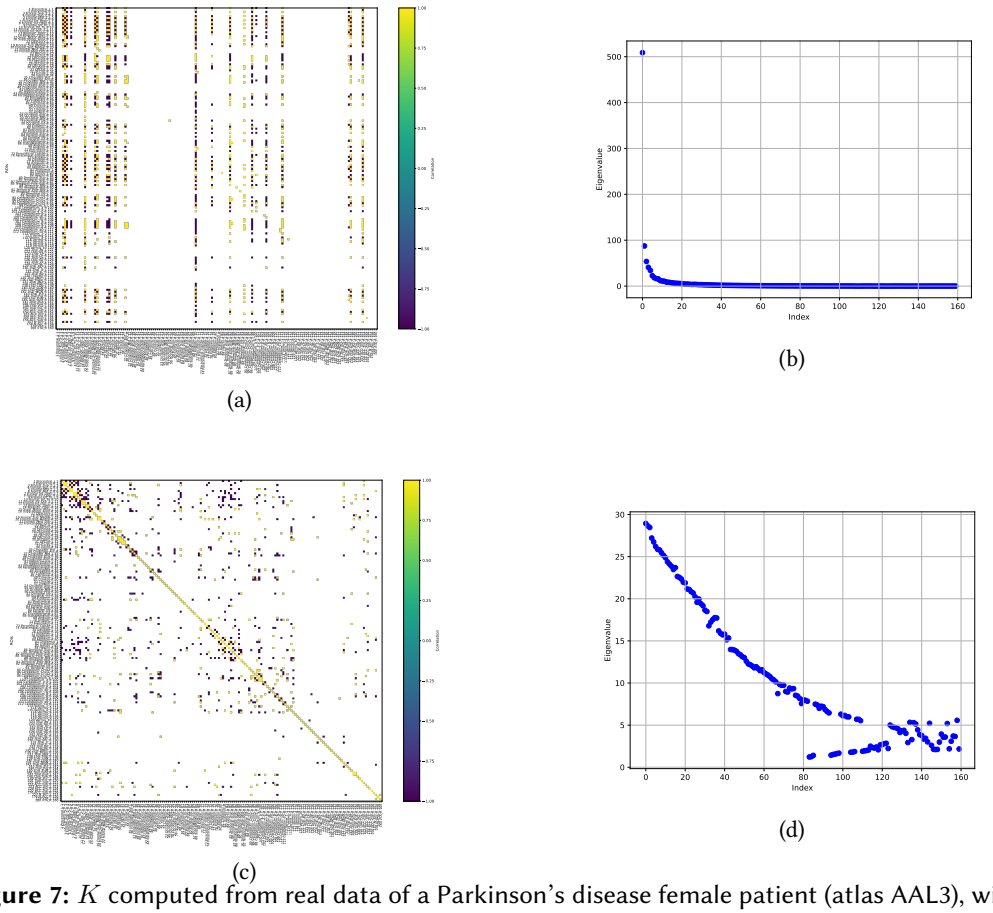

(a) (b) (c) (d)

Figure 7: K computed from real data of a Parkinson's disease female patient (atlas AAL3), with row-by-column (a) and element-wise product (c), and the respective eigenvalues (b,d). In (a), the elements above 12 are shown; in (c), above 0.8. (a) and (c) are taken from [9].

We can see some similarities, especially concerning the eigenvalues, aside from the computation technique adopted to find K. In particular, we notice the prevalence of the first eigenvalues for both techniques. Nevertheless, the scarceness of data regarding a full trend of Parkinson's or Alzheimer-Perusini's disruption [4], above all about the first stages of the disease, prevents us from investigating the detail of the mathematical properties of the K-operator, which will be the object of future studies.

5. Discussion and Conclusions

In our study, we proposed a method to investigate the K-operator and its properties from a mathematical point of view, namely the computation of its eigenvalues and eigenvectors. We applied this to the matrix representing the compromised brain $\mathcal{G}^k$ and to the K-operators obtained with two different computational techniques, i.e., the element-wise multiplication and the row-by-column one. According to our results, we can find some analogies between the general matrices obtained through the two methods, above all for what concerns their eigenvalues. We applied such a technique to some real data as well, finding results similar to the theoretical ones. This leads us to think about a possible link between the two computational techniques, that could be further investigated through a perturbation-based approach, as we mentioned in Section 2.4. Some limits that could be overcome in future studies are that the matrices we used in our toy examples, Section 3.1, are simplified and fictitious. It would also be interesting to study and compare more real-life data to understand better to which extent the individual impact of a disease differs from its general consequences and to distinguish more classes of K-operators representing different diseases. Moreover, considering the differences between male and female brains' disease development, we could aim for a better understanding of the differences between their aging processes. Age is a risk factor for neurodegenerative diseases; further research should also address other risk factors, genetic conditions, and other kinds of data to analyze, such as EEG and MRI, in addition to the fMRI. Unfortunately, the availability of data, especially concerning the brains of healthy volunteers, is limited.

We have several open questions: for instance, we aim to find a general theoretical property underlying the K-operator obtained with different computational methods, that could justify the analogies between the patterns of eigenvalues that we noticed. For now, we focused on some mathematical details of the K-operator, obtaining a "photography" of K, that is, a specific form of the operator for a patient, and between two-time points, that means between the fMRI data collected in two different stages of the disease. The more data information we have, the better we can approximate the action of K across time, that is, approximating its form as a time-dependent operator. Then, we could also define its dynamics.

From the pioneering intuition leading to non-invasive neuroimaging to our progressive steps with the formalization and exploration of the K-operator, our article may help pave the way toward the new informative yet ethical investigation of the brain and its network-related diseases. **Hence, the final objective of this research is to establish a foundational framework for the development of predictive models pertaining to the progression of neurodegenerative diseases. The mathematical representation adopted could improve the performance of predictive models by giving some prediction rules, for example, depending on the stage of the disease, it could be applied to predict the timing and severity of the disease. Neurodegenerative diseases are a class of disorders characterized by the progressive degeneration of the nervous system's structure and function. This study aims to provide the basis for exploiting the potential inherent in integrating innovative representations of brain impairment with sophisticated machine-learning methodologies.**

Code availability

The code can be accessed at https://github.com/sofiafazio/K_operator_Jupyter_eigenavalues (DOI 10.5281/zenodo.14281405). For Section 4, see https://github.com/medusamedusa/K_operator_parkinson (DOI 10.5281/zenodo.14162649), patient B, #100006, atlas AAL3.

Data availability

The real data we analyzed are derived from the Parkinson's Progression Markers Initiative (PPMI) dataset, with the following licenses and restrictions: "Investigators seeking access to PPMI data must sign the Data Use Agreement, submit an Online Application and comply with the study Publications Policy. Requests to access these datasets should be directed to PPMI, https://ida.loni.usc.edu/collaboration/access/appLicense.jsp."

Acknowledgments

This paper was developed within the project funded by Next Generation EU – "Age-It – Ageing well in an ageing society" project (PE0000015), National Recovery and Resilience Plan (NRRP) – PE8 – Mission 4, C2, Intervention 1.3. The views and opinions expressed are only those of the authors and do not necessarily reflect those of the European Union or the European Commission.

References

[1] S. Sandrone, M. Bacigaluppi, M. R. Galloni, S. F. Cappa, V. Moro, M. Catani, M. Filippi, M. M. Monti, D. Perani, G. Martino, Weighing brain activity with the balance: Angelo Mosso's original manuscripts come to light, Brain 137 (2014) 621–633. doi:10.1093/brain/awt091. arXiv:2013 May 17.

[2] J. Royer, B. C. Bernhardt, S. Larivière, E. Gleichgerrcht, B. J. Vorderwülbecke, S. Vulliémoz, L. Bonilha, Epilepsy and brain network hubs, Epilepsia 63 (2022) 537–550. doi:10.1111/epi.17171.

[3] W. W. Seeley, Mapping Neurodegenerative Disease Onset and Progression, Cold Spring Harbor Perspectives in Biology 9 (2017) a023622. doi:10.1101/cshperspect.a023622.

[4] A. Fathian, Y. Jamali, M. R. Raoufy, the Alzheimer's Disease Neuroimaging Initiative, The trend of disruption in the functional brain network topology of Alzheimer's disease, Scientific Reports 12 (2022) 14998. doi:10.1038/s41598-022-18987-y.

[5] A. Pathak, D. Roy, A. Banerjee, Whole-brain network models: From physics to bedside, Frontiers in Computational Neuroscience 16 (2022). URL: https://www.frontiersin.org/journals/computational-neuroscience/articles/10.3389/fncom.2022.866517. doi:10.3389/fncom.2022.866517.

[6] M. Mannone, P. Fazio, N. Marwan, Modeling a Neurological Disorder as the Result of an Operator Acting on The Brain: A First Sketch Based on Network Channel Modeling, Chaos 34 (2024) 053133. doi:10.1063/5.0199988.

[7] M. Mannone, P. Fazio, N. Marwan, P. Ribino, K-operator as a predictor for Alzheimer-Perusini's disease, in: Proceedings of the HCist – International Conference on Health and Social Care Information Systems and Technologies, 2024, 2024, in press.

[8] I.-M. Adrian, K. Gabriel, S. Claudio, M. S. Diana, V. H. Françoise, D.-D. adn Sabine, S.-M. Dominique, Machine Learning Approach for Classifying Multiple Sclerosis Courses by Combining Clinical Data with Lesion Loads and Magnetic Resonance Metabolic Features, Front Neurosci. (2017). URL: https://pubmed.ncbi.nlm.nih.gov/28744195/.

[9] M. Mannone, P. Fazio, P. Ribino, N. Marwan, J. Kurths, A Brain Network Operator for Modeling Disease: A First Data-Based Application for Parkinson's Disease, European Physical Journal, Special Topics (2024). doi:10.1140/epjs/s11734-024-01345-6.

[10] J. Goodman, Scientific Computing, Fall 2022, http://www.math.nyu.edu/faculty/goodman/teaching/SciComp2022/index.html, 2022. Accessed: 2024-08-08.

[11] M. Jenkinson, C. F. Beckmann, T. E. Behrens, M. W. Woolrich, S. M. Smith, FSL, NeuroImage 62 (2012) 782–790. URL: https://www.sciencedirect.com/science/article/pii/S1053811911010603. doi:10.1016/j.neuroimage.2011.09.015, 20 YEARS OF fMRI.

[12] J.-D. Tournier, R. Smith, D. Raffelt, R. Tabbara, T. Dhollander, M. Pietsch, D. Christiaens, B. Jeurissen, C.-H. Yeh, A. Connelly, MRtrix3: A fast, flexible and open software framework for medical image processing and visualisation, NeuroImage 202 (2019) 116137. URL: https://www.sciencedirect.com/science/article/pii/S1053811919307281. doi:10.1016/j.neuroimage.2019.116137.

[13] R. E. Smith, J.-D. Tournier, F. Calamante, A. Connelly, Anatomically-constrained tractography: Improved diffusion MRI streamlines tractography through effective use of anatomical information, NeuroImage 62 (2012) 1924–1938. URL: https://www.sciencedirect.com/science/article/pii/S1053811912005824. doi:10.1016/j.neuroimage.2012.06.005.

[14] G. Kocevar, C. Stamile, S. Hannoun, F. Cotton, S. Vukusic, F. Durand-Dubief, D. Sappey-Marinier, Graph Theory-Based Brain Connectivity for Automatic Classification of Multiple Sclerosis Clinical Courses, Front Neurosci. (2016). URL: https://pubmed.ncbi.nlm.nih.gov/27826224/. doi:10.3389/fnins.2016.00478.